Average Neutron Total Cross Sections in the 3- to 12-Mev Region*

NORRIS NERESON AND SPERRY DARDEN
University of California, Los Alamos Scientific Laboratory, Los Alamos, New Mexico
(Received October 31, 1952)

An experiment is described for measuring average neutron total cross sections over the 3- to 12-Mev energy region. The neutron source is a collimated beam of fast neutrons emerging from the Los Alamos Fast Reactor, and the detector is a proton recoil ionization chamber which serves as a neutron spectrometer. The average energy spread of the measurements is around 10 percent, and the over-all accuracy of the cross-section determinations is ±10 percent or better. Total cross-section results are presented for H, Be, C, O, Al, Si, S, Fe, Cu, Zr, Pb, Bi, and U. Neighboring elements above Fe are observed to exhibit regularities in their total cross-section patterns.

I. INTRODUCTION

A SURVEY of average neutron total cross sections in the 3- to 12-Mev energy range has been carried out using a method outlined previously.[1] This report presents total cross-section results obtained for thirteen elements scattered throughout the periodic table. Most of the elements were selected on the basis that previous cross-section data were available as a check over part of the energy range. This procedure has provided comparisons with other total cross-section data and has given information on the accuracy, resolution, and general reliability of the present method. This type of average cross-section information will be useful for checking theories treating the variation of total cross section with energy.

II. NEUTRON SOURCE

The neutron source in these experiments is the Los Alamos Fast Reactor.[2] This reactor possesses ports from which collimated beams of fast neutrons can be obtained. These beams have a maximum diameter of about 1 inch, are collimated to within 1°, and possess cadmium ratios of 1.00±0.01 as observed with a U^{235} foil. Above 2 Mev the energy spectrum of the neutrons emerging from these ports is similar to that of a fission neutron spectrum, i.e., the neutron flux decreases exponentially with energy such that approximately every 3 Mev the intensity diminishes by a factor of 10. For example, at a reactor power of 20 kw, the collimated neutron flux at an energy of 3 Mev is 5×10^6 neutrons cm^{-2} sec^{-1} Mev^{-1}, while at 10 Mev the corresponding flux is 3×10^4.

By using a neutron spectrometer type of detector the continuum of neutron energies present in the reactor beam can be converted into pulses whose heights are proportional to the neutron energies. The resulting pulse-height distribution can then be recorded on a multichannel pulse-height analyzer where each channel represents a small neutron energy interval. If an absorber is inserted in the beam, the transmission and total cross section of the material can be determined as a function of neutron energy.

The rapid decrease of the neutron flux with energy sets an upper energy limit to the method at about 13 Mev; above this energy the reactor neutron flux is so small that excessive running times are required to obtain adequate statistical accuracy. At energies below 12 Mev, it is possible to attain 5 percent statistics on cross-section determinations within several hours. A lower energy limit of 3 Mev was selected in this cross-section survey since a considerable amount of cross-section data have already been obtained with better resolution below an energy of 3 Mev.

III. DETECTION SYSTEM

A. Ionization Chamber

The neutron spectrometer detector is a parallel plate ionization chamber. The chamber operates directly in the collimated neutron beam from the reactor port. A radiator containing hydrogen or deuterium[3] (polyethylene) is used to convert the neutrons into proton or deuteron recoils. A platinum collimator immediately following the radiator allows the collimated particles emerging up to 10° of the forward direction to enter

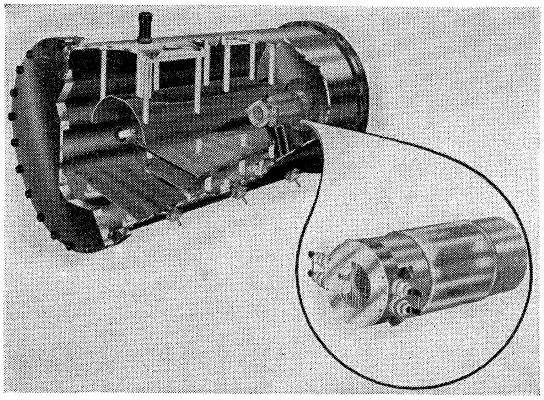

FIG. 1. Perspective view of ionization chamber.

* This work was performed under the auspices of the U. S. Atomic Energy Commission.
[1] N. Nereson, Phys. Rev. 87, 221 (1952).
[2] Rev. Sci. Instr. 18, 688 (1947).
[3] The polyethylene with its hydrogen replaced by deuterium was prepared by Dr. Anthony Ronzio of this Laboratory.

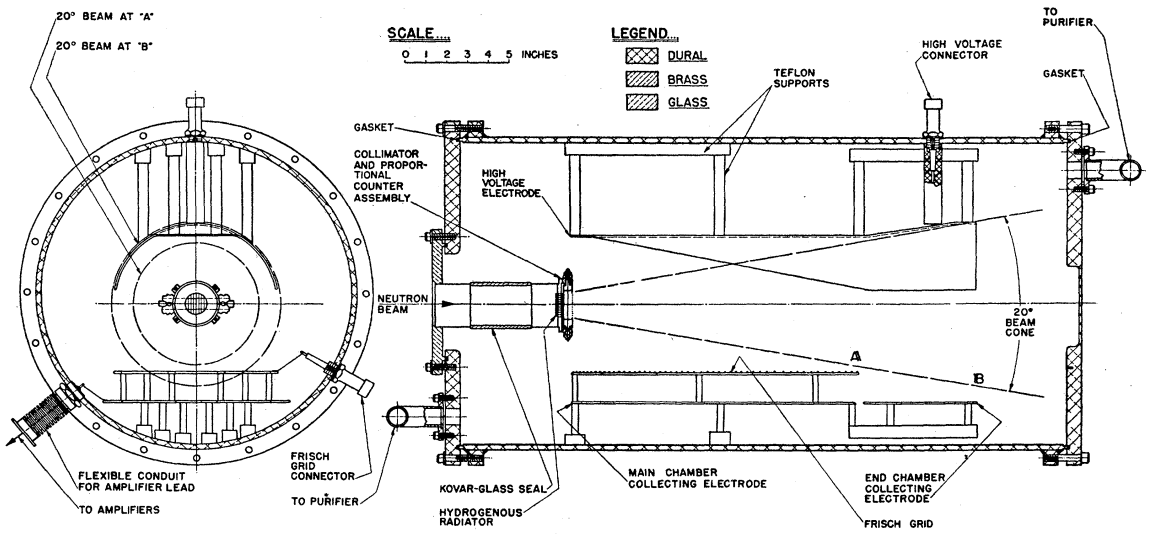

FIG. 2. Front and side views of ionization chamber.

the chamber volume. The energies of these collimated proton or deuteron recoils are determined by measuring their pulse height in a parallel plate ionization chamber equipped with a Frisch grid. In order to reduce background effects, the charged particles first pass through a small proportional counter before entering the main chamber volume. The proportional counter signal is operated in coincidence with the main chamber signal. However, only the pulse height from the main chamber is measured; the energy deposited by the recoil particles in the collimator and proportional counter is only a few percent of their total energy and can be calculated with sufficient accuracy. In order to avoid measuring recoils which leave the main chamber volume, another separate electrode is used which immediately follows the main collecting electrode. The signal from this end electrode operates in anticoincidence with the coincidence signal obtained from the main chamber and proportional counter.

A perspective view of the chamber is illustrated in Fig. 1, and front and side views are given in Fig. 2. The high voltage or top electrode is curved in order to increase the probability of the electrons being directed toward the grid rather than the outer walls of the chamber. Both collecting electrodes operate at ground potential. The shape of the collecting, grid, and high voltage electrodes is in the form of a trapezoid whose width is about 1 in. greater than that of the emerging proton beam. The main reason for this particular shape is to reduce the capacity of the collecting electrodes. In the present design, the capacities of the main chamber and end chamber are 35 $\mu\mu$f and 20 $\mu\mu$f, respectively.

The length of the collecting electrode is designed so that useful signal output is secured over a factor of two in neutron energy using one type of recoil particle with one gas filling. By a combination of proton and deuteron radiators, a factor of three in neutron energy can be covered with one gas filling. For example, at an absolute pressure of 40 psi the neutron energy range from 4.5 to 13.5 Mev can be investigated. The gas filling has usually consisted of a mixture of welding argon plus 2 percent carbon dioxide. With the above gas filling, the average time for the pulse from the main chamber to reach maximum height is about 1 μsec.

A weak Pu^{239} alpha-source, permanently mounted on the high voltage electrode, serves as a check on the operation of the chamber and amplifier in addition to calibrating the pulse height in terms of energy. A deposition of 5 Mev of energy in the main chamber gives a pulse height which is about 25 times the rms noise level of the amplifier system. A pulse-height distribution curve from this alpha-source gives a total width of about 3 percent at half-maximum height. This width is almost entirely due to amplifier noise and,

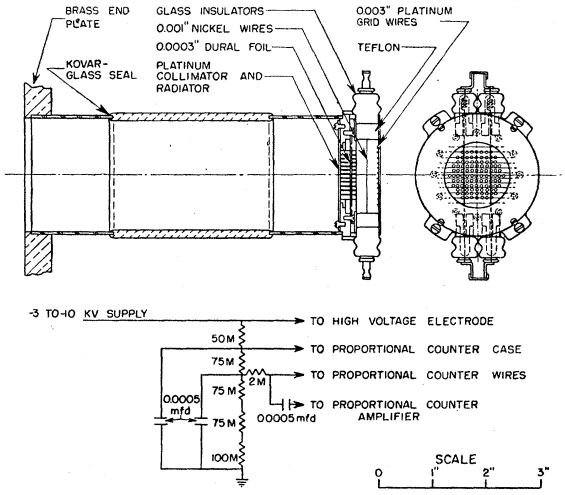

FIG. 3. Detail of collimator and proportional counter.

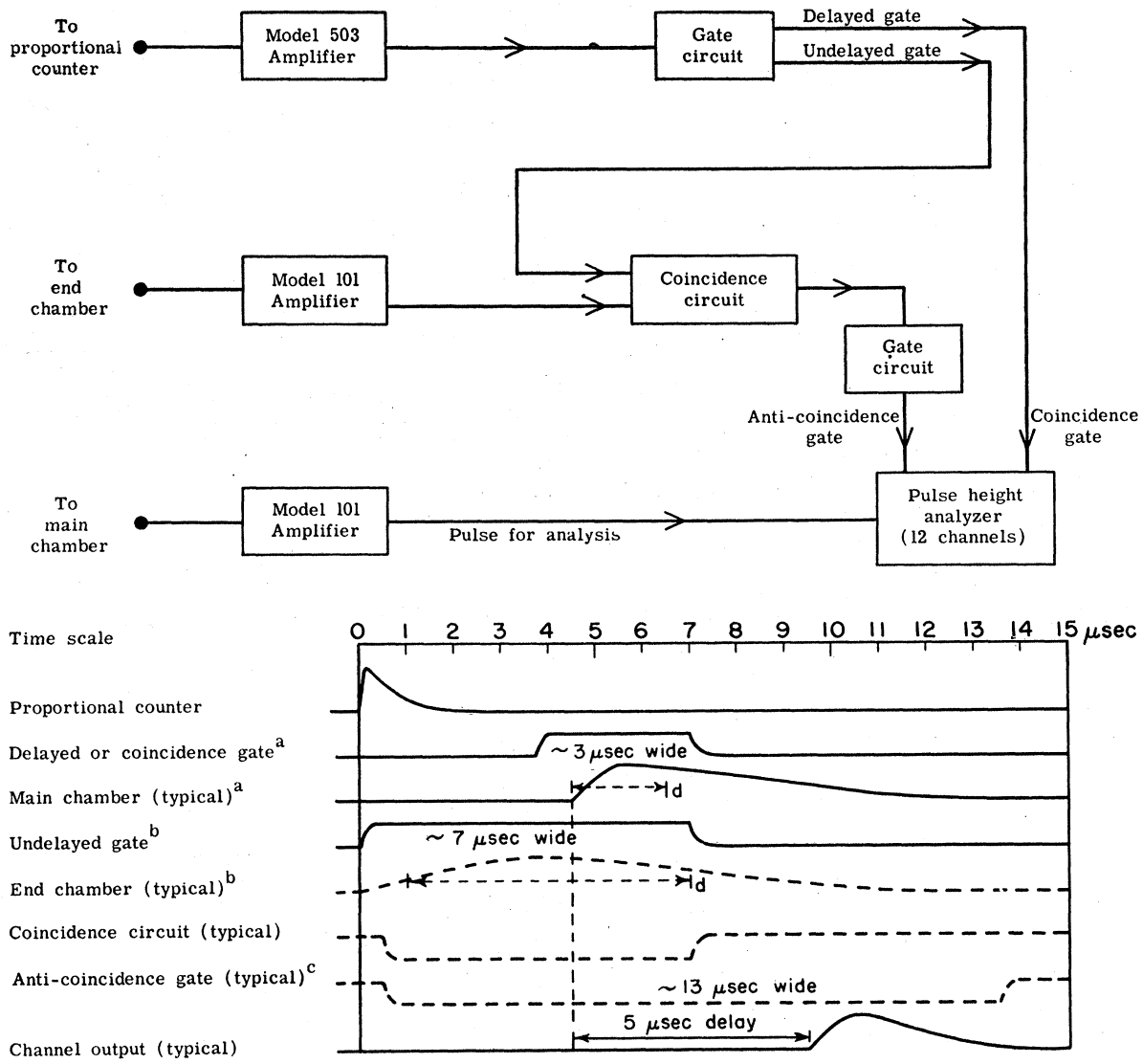

FIG. 4. Instrumentation and pulse shapes associated with ionization chamber. a. Coincidence between these two signals necessary for analyzer to count; b. coincidence necessary for anti-coincidence gate output; c. occurrence of this gate prevents analyzer from counting; d. dotted lines show approximate range of pulse-height peaks.

consequently, would be expected to increase with decreasing energy. In its present design, the chamber has been mainly used for neutron energies above 3 Mev. The practical lower energy limit of the present chamber design is about 2 Mev.

The alpha-source on the top electrode was used to determine the saturation characteristics and proper operating potentials for the chamber. Curves of pulse height *vs* top electrode potential (V_p) at a fixed grid potential (V_g) show a rising characteristic followed by a broad maximum. This maximum region is undoubtedly due to the variation of electron drift velocity in the argon-carbon dioxide gas mixture.[4] The same maximum value of alpha pulse height was observed at all pressures below 40 psi. However, at 49 psi the curves show the saturation pulse height is 3 percent less than at the lower pressures; a 4 percent decrease in maximum pulse height was observed at a pressure of 57 psi. Apparently electron attachment begins to have a noticeable effect at the higher pressures. The curves of pulse height *vs* V_g at a fixed V_p also show a rise followed by an extended maximum. The center of this maximum region occurs at about $V_g = V_p/4$, and the chamber was usually operated at this grid potential value. The potential which would normally exist at the position of the grid due to V_p alone amounts to $V_p/5.5$. A conventional calcium purifier maintained continuously at a temperature of 275°C keeps the pulse height constant. A

[4] See, for example, E. Klema and J. Allen, Phys. Rev. 77, 661 (1950).

representative example for a fixed gas filling shows that the alpha pulse height did not deviate more than ±0.5 percent during two months of operation.

A detail of the collimator and proportional counter assembly is illustrated in Fig. 3. The collimator consists of about 250 holes, each 0.047 inch in diameter, drilled with a 1 inch diameter circle in a 0.27 inch thick piece of platinum. The collimator is divided into two parts with a 0.0003-inch dural foil sandwiched between the two pieces. The dural foil serves as a pressure seal and thin window for admitting the proton or deuteron recoils to the chamber. This construction has the advantages of permitting radiators to be exchanged or removed on the exterior of the chamber and of not disturbing the gas filling during this procedure. In order to reduce background counts, i.e., counts obtained with the radiator removed, it is essential to remove all traces of grease and organic material from the collimator.

The small proportional counter following the collimator consists of two wires 1 mil in diameter mounted between two plane surfaces spaced 1 cm apart. One of these surfaces is the inside face of the collimator, and the other surface consists of a wire grid mounted on a platinum ring. The grid wires define the field of the counter and permit the recoil particles to pass through the interspaces into the main chamber.[5] Two collecting wires were used in order to insure adequate field strength over the entire collimator area. The counter multiplication depends upon the particular pressure and voltage in use and varies over a range from 5 to 20.

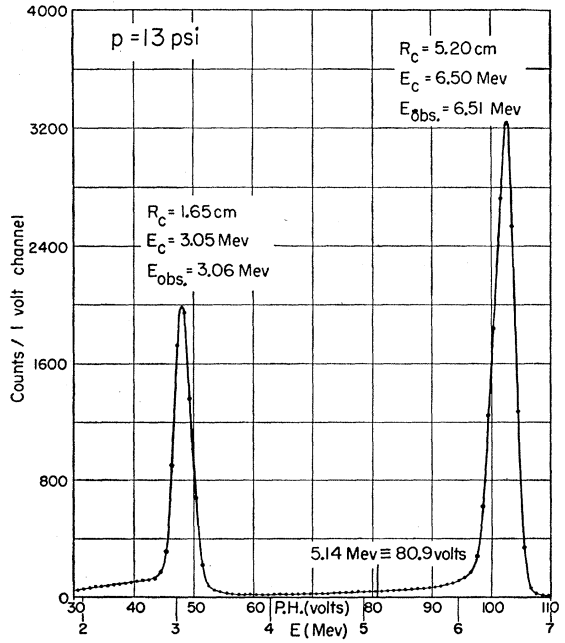

FIG. 5. Pulse-height distribution obtained from chamber with an alpha-source placed in front of collimator.

[5] The twelve platinum grid wires occupy 3 percent of the area which the protons recoils pass through.

The total rise time of the proportional counter signal is about 0.1 μsec for an argon—2 percent carbon dioxide gas mixture. As shown in Fig. 3, the potentials for this counter are derived from the main chamber high voltage supply.

The various electronic units and pertinent signal shapes associated with the ionization chamber are diagrammed in Fig. 4. A 12-channel pulse-height analyzer[6] is used to sort out the pulses from the main amplifier. The analyzer can register a count only during the occurrence of a coincidence gate signal which is initiated by the proportional counter. The delay and width of this gate is adjusted to coincide with the signals from the main chamber. The actual delay and time spread of the main chamber signals vary with the particular pressure and voltage in use on the chamber, but these factors can easily be ascertained by oscilloscope observation. Usually, the width of the gate is adjusted to approximately 3 μsec since the time spread of the main chamber signals averages about 2 μsec.

The analyzer cannot register a count during the period of an anticoincidence gate which is initiated by the end chamber. The end-chamber anticoincidence signal must logically occur shortly after a proportional counter signal; this is assured by having the end-chamber signal in coincidence with an undelayed gate produced by the proportional counter. The analyzer circuit delays each analyzed signal by 5 μsec before the signal goes to the scaler units. This is advantageous in the present case since late anticoincidence gates produced by protons near the high voltage electrode have ample time to nullify the channel output signal.

B. Check with Alpha-Particles

Preliminary testing of the chamber was carried out by placing an alpha-source at the position normally occupied by the radiator. The alpha-source consisted of the active deposit of thorium; this source has a half-life of 10.6 hours and emits two main alpha-groups having energies of 8.776 and 6.054 Mev. The source was deposited within a 1-in. diameter circle on a platinum disk. With the source placed 0.15 in. away from the front face of the collimator, the pulse-height distribution shown in Fig. 5 was obtained. The designations R_c and E_c refer, respectively, to the range and energy of the alpha-particles in the main chamber and were calculated from standard range-energy curves.[7] The energy E_{obs} is the main chamber energy calculated from the above pulse-height distributions using the 5.14-Mev alpha-source for a pulse height *vs* energy calibration. The values of E_c and E_{obs} are in good agreement which proves: (1) the main chamber collects all of the ionization produced beyond the grid wires of the proportional counter, and (2) it is satisfactory to use an alpha-source

[6] Wilkin Johnstone of this Laboratory is responsible for the design of the multichannel analyzer and gating circuits.

[7] Aron, Hoffman, and Williams, Atomic Energy Commission Report AECU-663 (1949), unpublished.

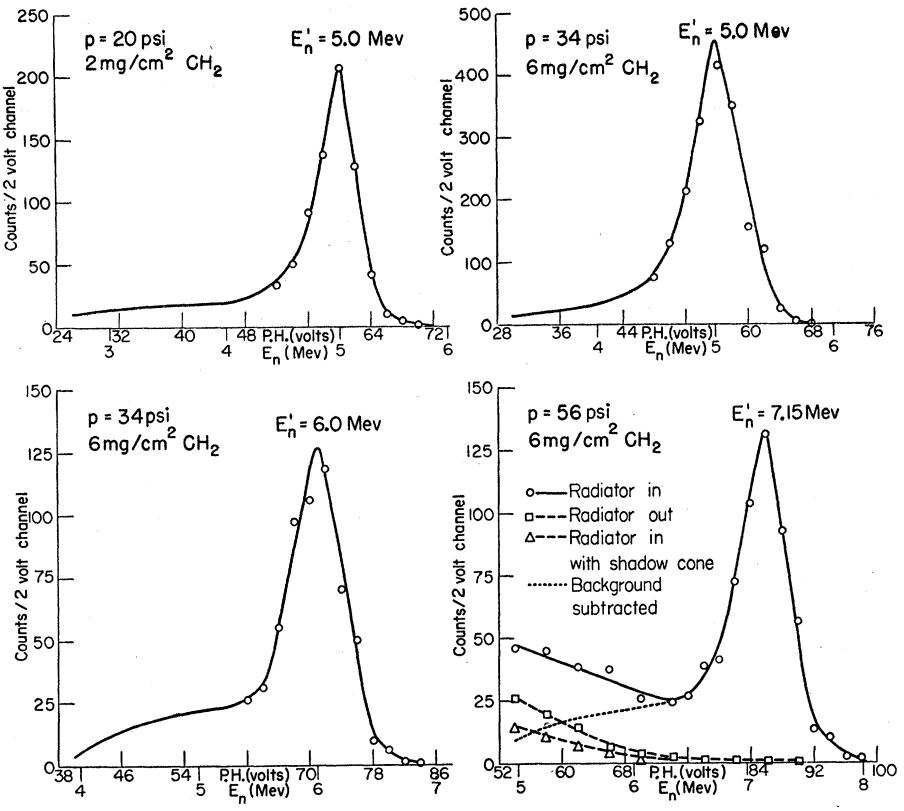

FIG. 6. Chamber pulse-height distributions obtained from monoergic neutrons.

mounted on the high voltage electrode as an energy standard for determining the energy deposited in the main chamber by particles arriving from the collimator.

The alpha-particle distributions show a total width at half-maximum of 7.5 percent and 4 percent, respectively, for the low and high energy distributions. Since the width of the 5.14-Mev alpha-source on the high voltage electrode is about 3 percent, the larger widths for the collimated alphas mainly arise from energy straggling in the collimator, dural foil, and proportional counter. The energy spread is less when the collimated particles deposit a greater fraction of their total energy within the main chamber volume, e.g., when the chamber is operated at a lower pressure. Another factor which broadens the energy spread at lower energies is the noise level of the amplifier; at low energies the noise level is a larger fraction of the pulse height than at the high energies.

The collimated alpha-particle distributions exhibit low energy areas which amount to 12 and 18 percent respectively of the total areas under the high and low energy distribution curves. The alpha-source on the high voltage electrode does not show the above effect. Since similar low energy regions are observed in the distributions for collimated protons and deuterons, it seems reasonable to conclude that these extraneous low energy particles are produced in the collimator. Their source probably arises from the original particles penetrating the edges of the collimating tubes or being scattered by the walls of the collimating holes.

C. Check with Neutrons

It seemed essential to test the chamber with monoergic neutrons in order to duplicate the actual conditions in which the chamber would be used. A Los Alamos electrostatic accelerator, utilizing the *d,d* reaction, provided a monochromatic source of neutrons within the 5-Mev to 7-Mev energy range. In all of these tests the radiator was located 8.5 in. from the end of the deuterium gas target of the accelerator. The target pressure was usually about 6 psi absolute; this pressure gave a total neutron energy spread ranging from 0.3 to 0.2 Mev for the 5- to 7-Mev range. The chamber was filled with the customary filling of welding argon plus 2 percent carbon dioxide. Irradiations were made with chamber pressures varying from 20 to 57 psi absolute and with polyethylene foil radiators in the 2 to 10 mg/cm² region. The bias on the proportional counter gate circuit was adjusted for normal operation, i.e., set slightly lower than that required to detect those protons traveling the full range of the main collecting electrode.

Typical results of the neutron bombardments are illustrated in Fig. 6 where the number of main chamber pulses in 2-volt channels are shown as a function of pulse-height and neutron energy. The energy E_n is the neutron energy calculated from the 5.14-Mev alpha-

source standard and other chamber constants, while E_n' is the neutron energy derived from the d,d source. Out of a total of ten irradiations the peak of the chamber pulse-height (or energy) distributions always agreed within 1 percent with the energy derived from the accelerator source. When obtaining the neutron or proton recoil energy from the alpha-source pulse height, it is important that the chamber is operated at saturation voltage for the alpha-particles.

The curves in Fig. 6 have a total width at half-maximum which ranges from 9 to 11 percent of the mean neutron energy; this is consistent with the expected width. For example, with a polyethylene radiator of 6 mg/cm^2 at a neutron energy of 6 Mev, the following quantities contribute to the resolution width: (1) the radiator gives a total energy spread of 8 percent, (2) the gas target on the accelerator produced an energy spread of 4 percent, (3) amplifier noise and chamber collection characteristics show a combined width of 3 percent as determined by the alpha-source pulse distribution, (4) the angular divergence of the protons from the collimating holes produces an energy width of about 2 percent, (5) the analyzer channel width of 2 volts contributes a width of 3 percent, and (6) proton energy straggling in the collimator, dural foil, and proportional counter probably contributes about 1 percent to the width. The resultant width of the above six contributions is slightly over 10 percent which agrees with the experimental result in Fig. 6. Since the radiator is responsible for the largest contribution to the energy width, the resolution can be improved slightly by using a thinner radiator. For example, with a 3 mg/cm^2 radiator at 6 Mev, the energy spread from the radiator is 4 percent and the expected resultant width would be about 8 percent; experiments verify this value.

All of the curves except one are shown with background effects subtracted. Two types of chamber background were experimentally measured: (1) that obtained with the hydrogenous radiator removed, and (2) that resulting with the radiator in place when a polyethylene shadow cone was placed between the target and radiator. The exact source of these background contributions is not known but it seems probable that the first type of background arises mainly from organic matter present on the inside face of the collimator and also from n,α reactions in the argon gas. The second background effect is most likely caused by neutrons being scattered into the radiator by the large frontal surfaces of the chamber. Typical magnitudes of the above two background effects obtained with the accelerator source are shown in the lower right corner of Fig. 6. These background curves represent upper limits since subsequent experiments showed that the first type of background can be reduced by a better cleaning of the collimator, and both types of background were improved by using delay line clipping instead of RC clipping on the main chamber pulses. Little effort was directed towards securing the lowest possible chamber background since in the practical application of the chamber these background effects were small and usually did not enter directly into the measurements.

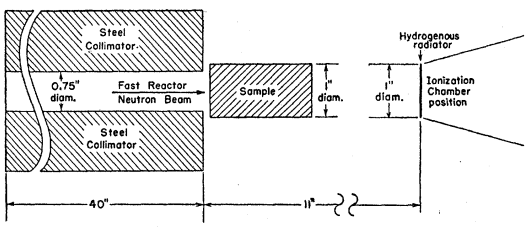

FIG. 7. Experimental arrangement for measuring neutron total cross sections.

The curves in Fig. 6 show an extraneous low energy region which comprises about 25 percent of the total proton recoils. As in the case with alpha-particles, these low energy recoils are believed to arise from protons being scattered by the collimator walls or protons penetrating the edges of the collimating holes. Scattering effects would be expected to decrease with energy whereas penetration effects would increase with the energy and range of the particle. Deuteron radiators instead of proton radiators have been used at neutron energies above 7 Mev in an attempt to diminish penetration effects. Unfortunately, no monoergic neutron checks using deuteron radiators in the chamber have been made since these radiators were not available at the time of the accelerator tests.[8]

The presence of the low energy component in the energy distributions of Fig. 6 is the main reason why the present chamber design is not suitable as a general fast neutron spectrometer. The above effect probably could be minimized by designing a collimator with a smaller ratio of wall surface to hole area.[9] Also, the use of deuteron recoils will improve the distribution.

The present ionization chamber detector is well suited for use with a fission type neutron spectrum. In this type of spectrum the extraneous low energy component produced in the platinum collimator is a smaller percentage of the total neutron intensity than in the case of a monoergic source. For example, using the

[8] Supporting experiments have been carried out using the electrostatic accelerator as a 6.3-Mev neutron source, a proton or deuteron radiator followed by an identical collimator to that used in the chamber, and a nuclear plate as a detector. The resulting recoil distributions showed (1) no low energy area with the collimator removed, (2) a 25 percent low energy region with the collimator and proton radiator, and (3) a 20 percent low energy region with the collimator and deuteron radiator. These experiments proved that an improved distribution curve is obtained with deuteron recoils and that the collimator itself (rather than some part of the main chamber) is entirely responsible for the energy degradation effect.

[9] The simplest way to accomplish this is to employ larger collimating holes so recoil particles could emerge at angles greater than 10°. This change would also aid in increasing the intensity of the recoils but would demand further separation of the chamber electrodes as well as increasing their width. Another suggestion is to make the collimating holes taper toward the center, i.e., have an hour-glass shape.

6-Mev energy distribution curve of Fig. 6 and a neutron spectrum which decreases exponentially by a factor of 10 every 3 Mev, a calculation shows that this low energy contribution is about 15 percent of the total proton recoil intensity at 6 Mev.

Other background effects associated with the above spectrum can be measured experimentally with the fast reactor neutron beam. First, the background obtained with the proton radiator removed is a maximum of 8 percent at energies around 3 Mev and decreases to a minimum of 2 percent at energies around 13 Mev.[10] With a deuteron radiator, the above background figures are reduced by a factor of two. This background is observed with the coincidence gate rate adjusted to the same value as with the radiator in place. The latter procedure is followed in order to include accidental coincidences in this same background figure. The ungated main chamber counts increase only by 20 percent when a radiator is inserted and, as a result, the accidental counts do not decrease appreciably with the radiator removed provided that the coincidence gate rate is adjusted to its normal value. The accidental counts comprise about one-third of the above background percentages and are determined by setting the delay of the coincidence gate at a large time value like 20 μsec or longer. Second, the background arising from neutrons scattered by the chamber walls into the radiator is negligible. This was checked by inserting a 10-in. length of polyethylene in the beam and noting that the observed small intensity corresponded to the transmission expected from this absorber length.

A check on the operation of the chamber in the fast reactor neutron beam consisted of verifying the exponential absorption law for neutrons. The chamber counting rate was observed as various thicknesses of carbon were placed in the beam. The results show that the intensity varies exponentially with carbon thickness down to transmissions of about 0.25. Below transmissions of 0.25, the observed values lie about 1 to 2 percent above the line determined by the previous points; evidently, multiple-scattering effects begin to appear in the results obtained with long absorbers. In order to minimize multiple-scattering effects, total cross-section measurements are made with absorbers having transmissions greater than 0.3 (usually 0.5).

IV. TOTAL CROSS SECTIONS

A. Experimental

The experimental arrangement for measuring neutron total cross sections is illustrated in Fig. 7. Since the majority of neutrons originate just beyond the far end of the steel collimator, the neutron source is about 40 in. distant from the sample. The experimental geometry on the source side of the sample is therefore very good,

[10] This background, when expressed in percent, will vary with radiator thickness. The thicknesses used here were such that the energy spread from the radiator alone never exceeded 10 percent of the mean neutron energy.

TABLE I. Energy spread of entire detector system for different radiators.

Radiator	Neutron energy Mev	Energy resolution percent
2 mg/cm² CH_2	3.0	10.5
	6.0	5.5
6 mg/cm² CH_2	5.5	11.0
	8.5	7.0
7 mg/cm² CD_2	7.0	13.0
	10.5	8.0
16 mg/cm² CD_2	10.0	16.0
	13.0	11.0
25 mg/cm² CD_2	12.0	20.0
	14.0	15.0

but the geometry on the detector side is only fair. When the above geometry is used, the correction for inscattering in the light elements can be neglected, since it does not exceed 0.6 percent for energies below 12 Mev. For the heavy elements, this correction amounts to a maximum of 1.3 percent at 12 Mev.[11] All of the absorbers employed were checked for uniform density and were at least 98 percent pure.

In a typical cross-section measurement the open beam intensity I_0 and the intensity I resulting with an absorber inserted in the beam are observed on the 12-channel analyzer over an energy interval of 3 to 4 Mev. The radiator is then removed,[12] and the corresponding background intensities I_{0b} and I_b are recorded. The transmission $T=(I-I_b)/(I_0-I_{0b})$ can then be obtained and the total cross section calculated for a maximum of 12 energy values. With certain radiators the percent background is the same for the open beam run as for the sample run (i.e., $I_b/I=I_{0b}/I_0$), and in this case it is not necessary to take background runs. A maximum numerical difference of 2 percent has been observed between background percentages taken with the open beam and with a sample.

Statistical reasons account for restricting a given set of data to a 3- or 4-Mev energy interval. The neutron source intensity decreases by a factor of 20 every 4 Mev and the cross section of hydrogen diminishes by approximately a factor of 1.5 over this energy interval. Therefore, if a cross section is measured to ± 1 percent statistical accuracy at the beginning of the interval, the corresponding accuracy at the end of a 4 Mev interval is approximately ± 8 percent. The data for next higher energy intervals are made to overlap the previous one, and the data for this interval are taken with a thicker radiator and a greater analyzer channel width in order to improve the accuracy at the end of the previous energy interval. The radiator thickness is usually chosen so that the energy spread of the entire

[11] Calculated from neutron diffraction scattering curves, B. Feld *et al.*, Atomic Energy Commission Report NYO-636 (1951), unpublished.

[12] More precisely, a blank piece of platinum is substituted for the radiator and its associated platinum backing. A $\frac{1}{32}$-in. thick piece of platinum precedes the radiator in order to prevent charged particles, created externally to the radiator, from entering the chamber volume.

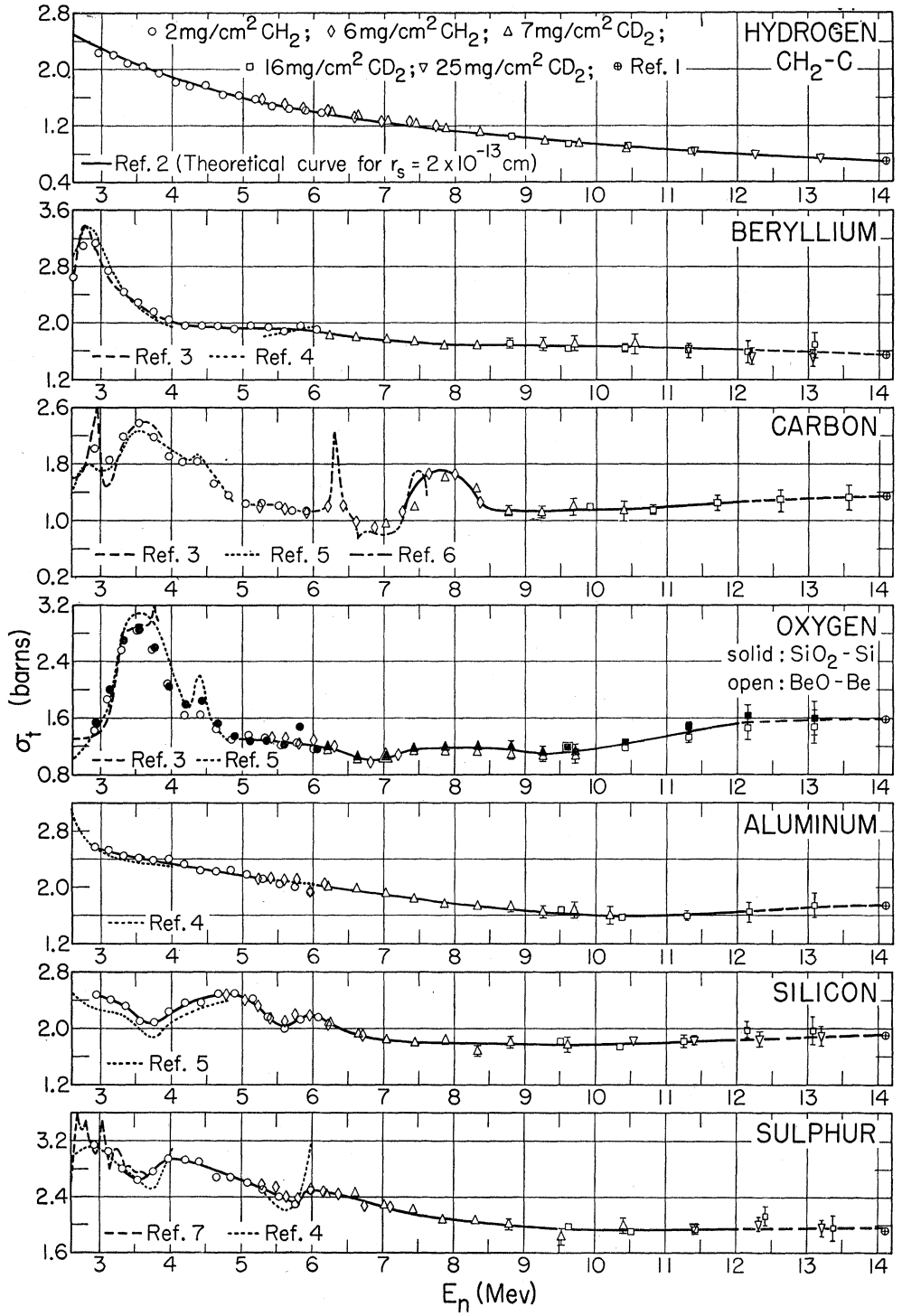

FIG. 8. Average neutron total cross sections of H, Be, C, O, Al, Si, and S. The references in the figure are (1) Coon, Graves, and Barschall, Phys. Rev. **88**, 562 (1952); (2) J. M. Blatt and J. D. Jackson, Phys. Rev. **76**, 18 (1949); (3) R. Ricamo and W. Zünti, Helv. Phys. Acta **8**, 419 (1951); (4) G. H. Stafford, Proc. Phys. Soc. (London) **A64**, 388 (1951); (5) Frier, Fulk, Lampi, and Williams, Phys. Rev. **78**, 508 (1950); (6) Los Alamos Electrostatic Accelerator Group, unpublished data, 1952; (7) R. Ricamo, Nuovo cimento **8**, 383 (1951); (8) Miller, Adair, Bockelman, and Darden, Phys. Rev. **88**, 83 (1952).

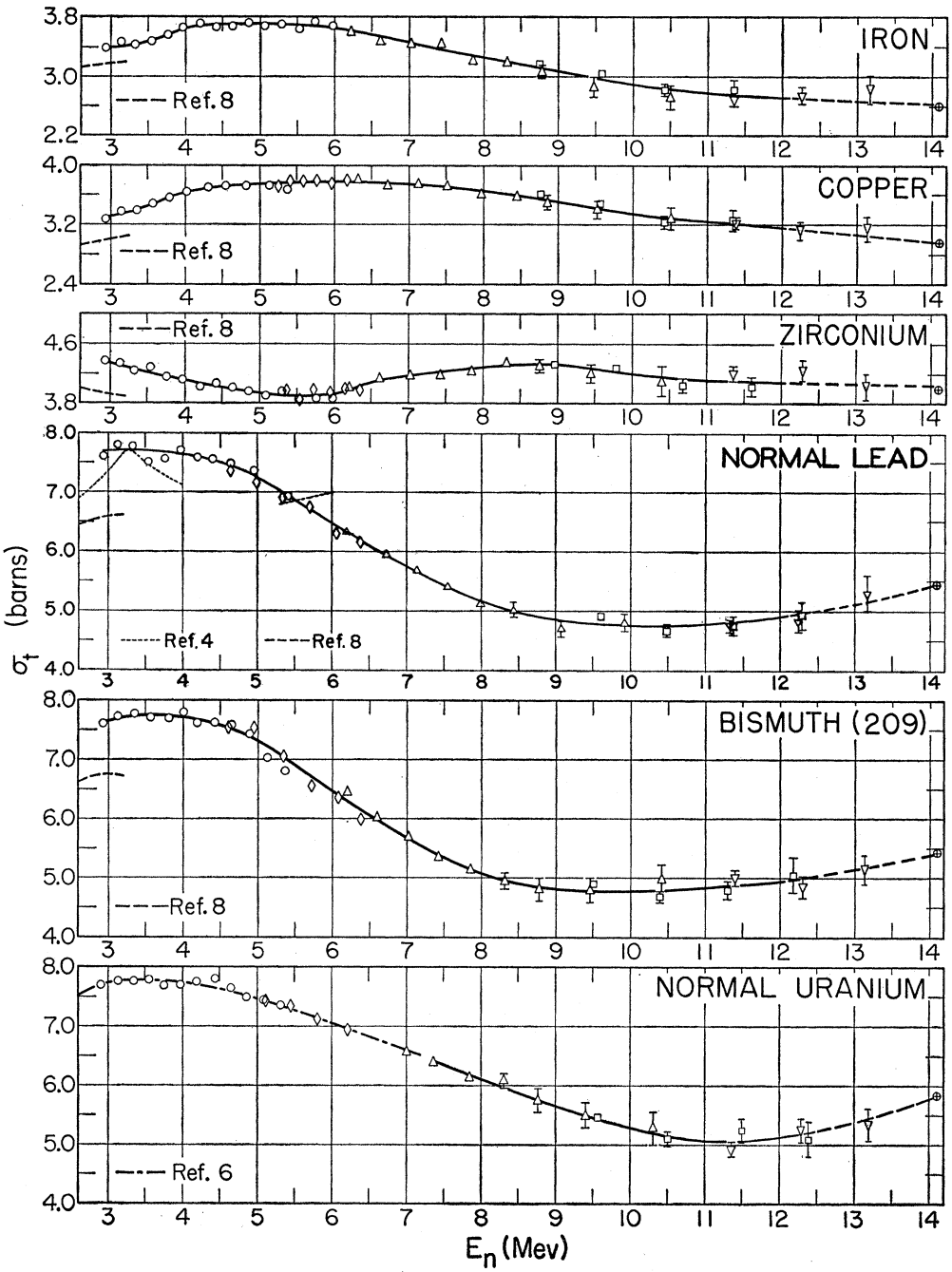

FIG. 9. Average neutron total cross sections of Fe, Cu, Zr, Pb, Bi, and U.

detector system is slightly greater than 10 percent at the beginning of the energy interval (see Table I). However, for neutron energies above 10 Mev the average energy spread has been increased to about 14 percent so as to obtain better accuracy in the 10–13-Mev energy region.

All of the radiator thicknesses listed in Table I are not always used in every cross-section determination. For example, the 6 mg/cm^2 CH_2 radiator is frequently omitted if the cross section does not vary rapidly in the 5.5 to 7.5-Mev energy region. Also, the 25 mg/cm^2 CD_2 radiator has been only used to obtain better statistical accuracy in the 12- to 14-Mev energy region. Although the present experiment is capable of providing only ± 5 percent statistical accuracy over the 3- to 12-Mev energy region, it is nevertheless useful to obtain a point around 13 Mev in order that the data can be extended closer to the 14.1-Mev value which is accurately known.

B. Results

The results of the measurements are shown in Figs. 8 and 9 where the average neutron total cross section σ_t is plotted against neutron energy E_n. The data obtained with the various radiator thicknesses are identified by separate symbols. A solid line representing the average cross section has been drawn through the present experimental points only in energy regions where better resolved data do not already exist. Where more accurate cross-section information is available, the points from the present experiment are plotted merely for comparison purposes. Since the present method gives poor statistical accuracy above 12 Mev, a dashed line over the 12- to 14-Mev region indicates that the cross-section behavior in this energy interval is uncertain. In conformity with the objective of measuring average cross sections, a smooth curve has been generally drawn through the data points rather than a detailed curve following small fluctuations. This procedure has been especially followed in regions where cross-section variations are smaller than the resolution of the measurements and where the errors are large, as over the 12- to 14-Mev range.

Hydrogen provides a good check measurement on an average cross section since this cross section contains no resonances and is well known. The hydrogen data were obtained by employing polyethylene and carbon absorbers. The results agree well with the theoretical curve of hydrogen for the case of the singlet effective range $r_s=2\times10^{-13}$ cm. It is interesting to note that a better fit can be observed for $r_s=2\times10^{-13}$ cm than for $r_s=1$ or 3×10^{-13} cm.

The resonances in the cross sections of beryllium and carbon provide information on the resolution of the present measurements. The wide resonances, such as the 3.6-Mev carbon resonance, are satisfactorily reproduced by the present method. The 2.75-Mev beryllium resonance (15 percent energy width) is not accurately followed near the peak of the resonance and therefore probably represents the limiting resolution of the method at this energy; this is consistent with the fact that the 2 mg/cm^2 CH_2 radiator contributes an energy spread of 14 percent at the above energy. The beryllium resonance check indicates that it is satisfactory to determine the energy resolution from the detector constants. Narrow resonances (2–3 percent energy width), such as the 6.3-Mev carbon resonance and the 4.4-Mev oxygen resonance, show as slight rises in the present measurements.

The carbon measurements are a representative example of how the present data average out the narrow peaks and dips in cross-section determinations using better resolution; however, in the energy regions where the carbon cross section does not fluctuate rapidly, the data agree well with the other measurements. The electrostatic accelerator check measurements indicate multiple structure is present in the large carbon resonance centering at 7.8 Mev. The low energy side of the above resonance demonstrates how the resolution is improved with the 6 mg/cm^2 CH_2 radiator over that of the 7 mg/cm^2 CD_2 radiator. In energy regions where cross-section results vary with energy, the better resolved values from the thinner radiator have usually been given preference to the more statistically accurate results from the thicker radiator.

The two sets of oxygen measurements were made by using the combinations beryllium oxide-beryllium and quartz-silicon. In regions where statistical errors are small, the differences between these two sets of measurements are probably indicative of the systematic errors present in this experiment, *viz.*, sample purity, sample measurement and weighing, amplifier drift, and analyzer instability. Except for three points, the two sets of data are in agreement within ±10 percent. It is difficult to understand why the data do not agree better with the high energy side of the oxygen resonance centering at 3.5 Mev; the discrepancy is in the wrong direction to be accounted for by poor resolution.

Except possibly for silicon and sulfur, no outstanding similarities in cross-section behavior are observed in the light element results of Fig. 8. It is interesting to note that both silicon and sulfur show cross-section minima in the energy regions of 3.5–3.7 and 5.6–5.8 Mev.[13] However, this common feature may be accidental rather than a regularity since the adjacent element, aluminum, does not show a similar pattern. More information on neighboring elements is needed to establish conclusive cross-section trends for elements in this region.

Common tendencies in average cross-section patterns of neighboring elements are much more evident for the heavier elements illustrated in Fig. 9. Both iron and copper possess broad maxima centering about 5 to 6 Mev and show a decrease in cross section at higher energies. Zirconium, removed from the above elements, shows an entirely different behavior, *viz.*, a minimum in the 5- to 6-Mev region and a considerably smaller percentage change in cross section at higher energies. The heavy elements, bismuth, lead and uranium, show the cross-section regularities of a broad maximum around 3.5 Mev, a rather rapid decrease from 5 to 9 Mev, a minimum in the 9.5- to 11.0-Mev region, and a slow increase towards 14 Mev. The above minimum appears to shift towards higher energies with increasing atomic number. (The lead cross-section measurements consistently showed a small dip at 3.5 Mev.)

The above results are similar to the cross-section regularities observed by Barschall[14] and by Miller and others[15] in the 0.1- to 3-Mev energy region. Further

[13] The second minimum is probably not resolved by the present measurements.

[14] H. Barschall, Phys. Rev. **86**, 431 (1952).

[15] Miller, Adair, Bockelman, and Darden, Phys. Rev. **88**, 83 (1952).

measurements are being carried out on additional elements as more information is desirable to confirm the cross-section trends observed for the present elements.

The authors wish to thank the electrostatic accelerator group for using their machine to check the ionization chamber detector and also for measuring the total cross section of carbon as a check on the present measurements. Edward Jurney of this laboratory assisted materially in the early development of the detector.

PHYSICAL REVIEW VOLUME 89, NUMBER 4 FEBRUARY 15, 1953

Cross Section for the Reaction $D(d,p)H^3$†

C. F. Cook and J. R. Smith*
Rice Institute, Houston, Texas
(Received October 31, 1952)

Cross sections for the reaction $D(d,p)H^3$ have been measured between 50 and 100 kev, using thin targets of deuterium absorbed in zirconium. With the angular distribution data of Wenzel and Whaling, the total cross sections have been calculated. The total cross section at 100 kev is measured to be 14.8 millibarns. A gas target was used to determine the cross section at 420 kev. The value obtained was 49.3 millibarns.

INTRODUCTION

MEASUREMENT of the cross section for the reaction $D(d,p)H^3$ has been the object of several experiments,[1–4] using both thick and thin targets. The present investigation utilizes thin targets of deuterium absorbed in zirconium films evaporated on to $\frac{1}{2}$-in. aluminum disks. Targets of this type have been successfully used to measure the d-T cross section, and the paper by Conner, Bonner, and Smith[5] discusses their preparation.

EXPERIMENTAL METHOD

The experimental apparatus used was essentially the same as that employed in measuring the d-T cross section at low energies, and the reader is referred to the earlier paper for details of the construction. The deuteron beam from the Cockroft-Walton accelerator was separated into its mass components and deflected 10° by a magnetic field. The beam was collimated by two $\frac{3}{16}$-in. diameter apertures, one of which was 10 cm above, the other 30 cm below the center of the $2\frac{1}{2}$-in. diameter pole faces of the magnet. Deuterons then struck the target at an angle of 20° to the normal. Disintegration protons were counted at an angle of 90° to the incident deuteron beam by a counter filled to a pressure of $\frac{1}{2}$ atmosphere with a mixture of argon plus 5 percent CO_2. The counter accepted protons in a solid angle defined by a 1.00-cm circular aperture located 7.64 cm from the center of the target. The solid angle was thus 0.01346 steradian. With a voltage of 1300 v on the counter, the bias curve showed a plateau 40 volts wide.

The number of incident deuterons was determined by measuring the charge deposited on the target with a current integrator of the type described by Watt.[6] Secondary electrons produced at the lower slit and at the target were electrostatically repelled to their respective origins. Correction for neutralized deuterons in the beam was made by taking a background count with the charged beam bent away from the target by a strong permanent magnet placed between the target and the lower slit. At the highest energies the neutral correction amounted to 2 percent; at 50 kev it was 4 percent.

The number of deuterium atoms per square centimeter of the Zr targets was determined by comparing the proton yield of each target with that of a deuterium gas target. The gas target is illustrated in Fig. 1. The deuteron beam from the Van de Graaff generator was defined by S' to be 5 mm in diameter and then entered the target through an aluminum foil having a thickness of 1.26 mg/cm². The energy of the deuterons incident on the foil was 800 kev. The energy loss in the foil was calculated from the data of Warshaw[7] to be 380 kev, so that the energy of the deuterons incident on the deuterium gas was 420 kev. Protons from the d-D reaction were counted at an angle of 90° to the beam by a counter consisting of thin anthracene flakes mounted on a 5819 photomultiplier tube. The solid angle was defined by aperture B, a $\frac{3}{8}$-in. hole covered with an aluminum foil 0.020 mm thick and located 4.4 cm from the center of the beam. When the yield of the gas target was to be determined, slit A, 0.626 cm

† This work was supported by the U. S. Atomic Energy Commission.
* National Science Foundation Predoctoral Fellow.
[1] Bretscher, French, and Seidl, Phys. Rev. **73**, 815 (1948).
[2] Moffat, Roaf, and Sanders, Proc. Roy. Soc. **A212**, 220 (1952).
[3] Arnold, Phillips, Sawyer, Stovall, and Tuck, Phys. Rev. **88**, 159 (1952).
[4] W. A. Wenzel and W. Whaling, Phys. Rev. **88**, 1149 (1952).
[5] Conner, Bonner, and Smith, Phys. Rev. **88**, 468 (1952).
[6] B. E. Watt, Rev. Sci. Instr. **17**, 334 (1946).
[7] S. D. Warshaw, Phys. Rev. **76**, 1759 (1949).

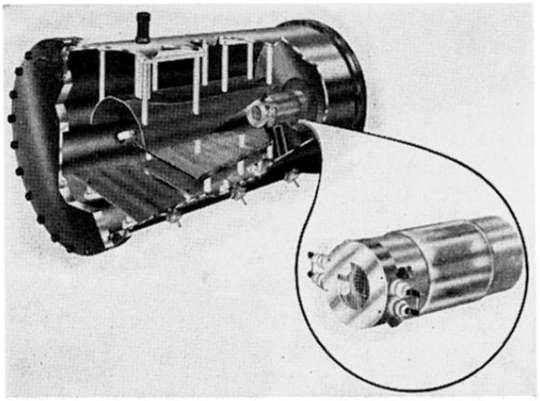

FIG. 1. Perspective view of ionization chamber.